
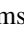













Selective Motion Artefact Reduction via Radiomics and k-space Reconstruction for Improving Perivascular Space Quantification in Brain Magnetic Resonance Imaging

Jose Bernal¹ , William Xu¹ , Maria d. C. Valdés-Hernández¹ ,
Javier Escudero² , Angela C. C. Jochems¹ , Una Clancy¹ , Fergus N. Doubal¹ ,
Michael S. Stringer¹ , Michael J. Thrippleton¹ , Rhian M. Touyz³ ,
and Joanna M. Wardlaw¹ 

¹ Centre for Clinical Brain Sciences, The University of Edinburgh, Edinburgh, UK
jose.bernal@ed.ac.uk

² Institute for Digital Communications, The University of Edinburgh, Edinburgh, UK

³ Institute of Cardiovascular and Medical Sciences, University of Glasgow, Glasgow, UK

Abstract. Current evidence points towards perivascular spaces playing a key role in cerebral haemodynamics and waste clearance. Hence, their precise quantification may become a powerful tool for assessing brain health and further establishing their relationship with neurological diseases. Large strides have been made towards developing automatic tools to computationally assess the burden of perivascular spaces in MRI in recent years. However, their applicability depends to a large extent on the quality of the images. In this paper, we propose a pipeline to improve perivascular space quantification by means of radiomics-based image quality control and selective motion artefacts reduction. We demonstrate our method on a sample of patients with mild stroke ($n = 60$) with different extents of small vessel disease features and image quality. We show our proposal can differentiate high- and low-quality scans (AUROC = 0.98) and reduce imaging artefacts, which leads to greater correlations between visual and computational measurements, especially in the centrum semiovale (polyserial correlation: 0.86 [95% CI 0.85, 0.88] and 0.17 [95% CI 0.14, 0.21] with and without our proposal, respectively). Our preliminary results demonstrate the potential of our proposal for retaining clinically relevant information while reducing imaging artefacts.

Keywords: Perivascular spaces · Cerebral small vessel disease · Image enhancement · Imaging artefact reduction · Brain magnetic resonance imaging

1 Introduction

Perivascular spaces (PVS) in the brain are the cavities surrounding perforating cerebral microvessels, serving as drainage conduits through which interstitial fluid clearance is facilitated [1]. If enlarged or dilated, they appear hyperintense on T2-weighted MRI

sequences [2]. Although first described in the mid-1800s, their potential significance as indicator of brain health has only emerged recently following advancements in imaging technology [3]. Nonetheless, their association and involvement alone with neurological risk factors and disease is still currently debated [3], hence the importance of assessing PVS quantitatively to validate their use as a neuroimaging feature.

The majority of studies on PVS rely solely on clinical visual ratings [1, 4]. Although qualitative PVS assessments are quick, easily interpreted, and replicable, they are limited by their discrete nature, as with many qualitative scoring methods. Attempts to automate the quantification of PVS, while partly successful, are limited by imaging artefacts [5]. The incidence of imaging artefacts impeding automatic PVS segmentation has peaked at 20% in large-scale studies [5]. Thus, reduction of imaging artefacts during pre-processing prior to PVS quantification is necessary to reduce research waste and increase reliability of study results. Nonetheless, the application of image enhancement techniques requires distinguishing between high- and low-quality input scans as filtering high-quality scans is detrimental to PVS sensitivity [6].

The assessment of image quality is a long standing and challenging problem. Even though image analysts could potentially visually inspect all acquisitions, the task is tedious, time-consuming and error-prone due to inter- and intra-observer variability, especially in large-scale studies [7]. In the field of PVS segmentation, automatic quality control has been successfully conducted via texture analysis [6]. However, the presence of brain pathologies may limit the effectiveness of such approaches as textures vary with the burden of neuroimaging features and imaging artefacts [8, 9].

In this work, we propose a framework that identifies and enhances scans distorted by motion artefacts via radiomics and k-space analyses prior to PVS quantification, thus reducing imaging artefacts compromising computational assessments while retaining clinically relevant patterns on high-quality acquisitions. We tested our proposal on a well-phenotyped cohort of patients with a history of mild stroke presenting various neuroimaging features of small vessel disease.

2 Materials and Methods

As illustrated in Fig. 1, we determine the quality of the input image automatically and, if it is distorted by motion, we enhance its quality before PVS segmentation.

2.1 Subjects, Magnetic Resonance Imaging and Clinical Visual Scores

T2-w scans were obtained from a sample of an ongoing prospective study (The Mild Stroke Study 3: ISCTRN 12113543) of patients with a recent mild stroke ($n = 60$; 24 women; median age 69 years [IQR 58–75]; age range 40 to 85 years) with a varied burden of neuroimaging features of small vessel disease. We used data from the first and second visit (60 and 35 scans, respectively, were available at the time). Approval for this study was obtained from South East Scotland Research Ethics Committee (Ref 18/SS/0044) and NHS Lothian Research & Development (Ref 2018/0084).

T2-w MRI was performed on a 3T MRI scanner (MAGNETOM Prisma, Siemens Healthcare, Erlangen, Germany) and a 3D axial SPACE T2-w imaging sequence (TR/TE = 3200/408 ms, $0.94 \times 0.94 \times 0.90$ mm acquired resolution, 24.0×24.0 cm field of view)¹. An experienced neuroradiologist provided visual clinical ratings for PVS in the basal ganglia and centrum semiovale for the entire sample following the Potter scale [1]. The distribution of scores in the sample can be found in Table 1.

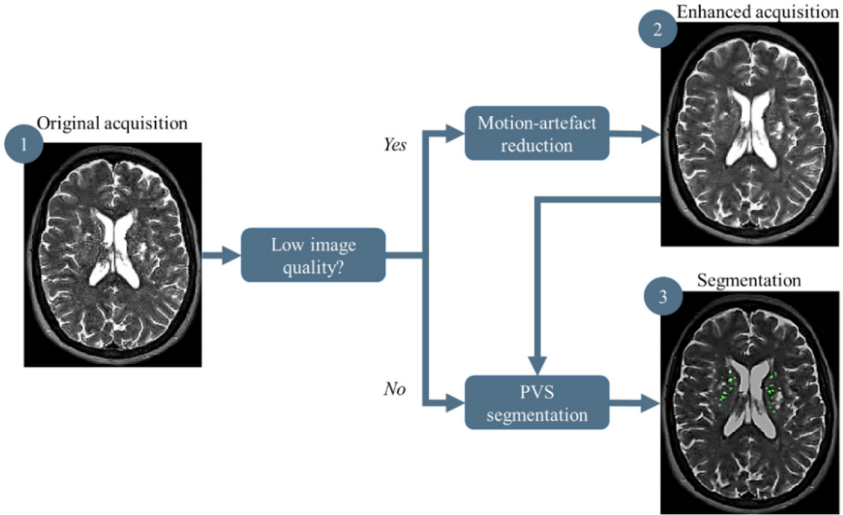


Fig. 1. Proposed pipeline for quantifying perivascular spaces in T2-w scans. We evaluate the quality of the scans, selectively correct frequencies that appear corrupted by motion, and segment perivascular spaces (detected perivascular spaces in green). (Color figure online)

Table 1. Distribution of clinical visual ratings for PVS in the basal ganglia and centrum semiovale in the MSS3 subsample. We report both frequencies and relative frequencies.

Rating	Basal ganglia	Centrum semiovale
0	0 (0%)	0 (0%)
1	16 (27%)	9 (15%)
2	26 (43%)	16 (27%)
3	18 (30%)	27 (45%)
4	0 (0%)	8 (13%)

¹ Full details of the study protocol and image acquisition are provided in [24].

2.2 Image Quality Assessment

Image quality metrics specifically designed for quantifying distortion due to noise and motion based on the analysis of background signal are suitable for image quality control as ghosting artefacts may be prevalent in this region and their values are unlikely to be indicative of the status of the brain. We tested four metrics accounting for noise and motion artefacts: the entropy-focus criterion, foreground-background energy ratio, mean background intensity, and signal-to-noise ratio (Table 2).

Table 2. Considered metrics for quantifying motion and noise in T2-w scans.

Image quality metric	Description
Entropy-focus criterion [10]	Entropy of voxel intensities as a measure of ghosting and blurring artefacts caused by motion. Lower entropy values may reflect lower motion artefacts
Foreground-background energy ratio [7]	Variance of voxel intensities in the intracranial region divided by that in background. The lower the ratio, the lower the image quality
Mean background intensity	Mean intensity in background. Higher values may be indicative of motion artefacts
Signal-to-noise ratio	Mean intensity in brain tissue divided by the standard deviation of intensities in background. The higher the ratio, the higher the image quality

The classification steps are as follows. Firstly, we extracted the aforementioned descriptors from each input image using the automatic MRI Quality Control tool² [7]. Secondly, we entered the resulting values in a logistic regression model to predict image quality (high-quality vs motion-corrupted). This model was trained using data from the second visit as described in Sect. 2.1 (9 motion-corrupted and 29 high-quality scans).

We validated our image quality control step against the classification of a trained analyst blind to our automatic assessment.

2.3 Motion Artefact Reduction

Once we separate high-quality and motion-corrupted images, we aim to reduce imaging artefacts on low-quality images, especially motion distortion.

Motion correction has been widely investigated [11, 12] and remains an unresolved challenge, although many partial solutions exist [11]. The applicability of motion reduction methods is dependant to a large extent on the availability of motion-tracking devices, prior information on the patient's movement, and the stage at which signal post-processing is applied (i.e., prospective or retrospective motion correction). In this particular case, we operate on the 'k-space' data obtained via Fourier transformation given the lack of the original k-space data or patient movement information.

² The MRIQC documentation can be found in mriqc.readthedocs.io.

Considering this, we decided to identify and compensate for inconsistencies in the ‘k-space’ data obtained via Fourier transformation of the T2-w images- sawtooth-like patterns depicted in Fig. 2. Assuming we can identify them appropriately (e.g., Fig. 2C, but not Fig. 2D), we can formulate motion reduction as a regression problem in which we estimate missing Fourier coefficients that increase image quality. In this work, we manually inspected k-spaces to select segments affected by sawtooth patterns.

Let $y : \mathbb{R}^3 \rightarrow \mathbb{R}$ be a motion-corrupted image. If we just nullify segments of the k-space displaying sawtooth patterns using an ideal low-pass filter M , the resulting image will be of greater visual quality in-plane, but of a poorer resolution in the superior-inferior direction compared to the original one. Instead, regress a new k-space $x^* : \mathbb{R}^3 \rightarrow \mathbb{R}$ that minimises the following expression

$$x^* = \underset{x}{\operatorname{argmin}} \gamma \|x - y\|_2^2 + \|M \star (x - y)\|_2^2 + \omega \|x\|_{TV}, \quad (1)$$

where \star denotes the convolution operator, $\omega, \gamma \in \mathbb{R}$ weighting parameters and $\|\cdot\|_{TV}$ the total variation semi-norm. Each term in the expression ensures that (i) the resulting image x^* appears similar to the original, (ii) frequencies that are not visually affected by motion artefacts are retained, and (iii) potential “ringing” artefacts are reduced, in that order. Following qualitative analysis, we found $\omega = 0.5$ and $\gamma = 0.01$ balanced improving image quality and minimising blurring. We used the package developed by Lustig et al. [13] for finding an x^* by means of conjugate gradient and line-search.

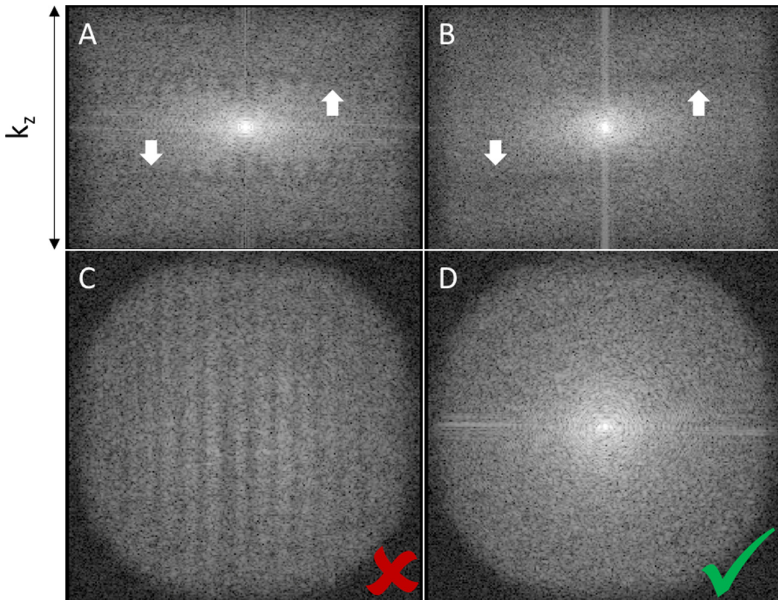


Fig. 2. Sawtooth-like patterns observed in the k-space of a motion-corrupted image. These patterns are visible in the slice direction kz in A and B (indicated by the white arrows) and in plane in C. Image D shows a slice visually free of artefacts.

2.4 PVS Segmentation

Most techniques segmenting PVS are based on eigenanalysis of the Hessian matrix as it encapsulates geometric properties used for distinguishing tubular structures (e.g., local curvature and eccentricity) [14]. The Hessian matrix H of a continuous and twice differentiable function $f : \mathbb{R}^3 \rightarrow \mathbb{R}$ is expressed as $(Hf)_{ij} = \partial^2 f / \partial x_i \partial x_j$. Digital images are typically convolved with multiple Gaussian kernels to ensure continuity and differentiability, and to enable multi-scale detection.

The eigenvalues of the Hessian matrix $\lambda_1, \lambda_2, \lambda_3$, with $|\lambda_1| \leq |\lambda_2| \leq |\lambda_3|$, characterises PVS in T2-w sequences since regions fulfilling $|\lambda_1| \approx 0$ and $\lambda_2 \approx \lambda_3 \ll 0$ are hyperintense tubular structures [14]. Moreover, complementary analysis permits targeting tubular objects with specific properties. For instance, the Frangi filter examines three additional properties $R_b = |\lambda_1| / \sqrt{|\lambda_2 \lambda_3|}$, $R_a = |\lambda_2| / |\lambda_3|$, and $S = \sqrt{\lambda_1^2 + \lambda_2^2 + \lambda_3^2}$ to filter blobs, lines, and low contrast structures, respectively [14, 15]. These three aspects are jointly evaluated in the vessel likelihood response as follows:

$$V = \begin{cases} 0 & \text{if } \lambda_2 > 0 \text{ or } \lambda_3 > 0, \\ \left(1 - e^{-R_a^2/2\alpha^2}\right) \left(e^{-R_b^2/2\beta^2}\right) \left(1 - e^{-S^2/2c^2}\right) & \text{otherwise,} \end{cases}$$

where α, β , and c control the sensitivity of the filter to the aforementioned properties. Parameter optimisation experiments have shown that default parameters ($\alpha = 0.5$, $\beta = 0.5$, and $c = 500$) work well for PVS segmentation [16].

2.5 Comparison Against a Relevant Framework

We compared each step of our proposal against that of a similar framework that attempts to evaluate image quality and correct imaging artefacts prior to PVS segmentation [6]. In that work, image quality was assessed via Haralick-based texture analysis; imaging artefacts corrected by means of the total variation denoising framework; and PVS segmentation using the Frangi filter.

2.6 Validation Against Clinical Parameters

We computed polyserial correlations to determine the strength of the relationship between visual and computational measurements of PVS.

3 Results

3.1 Image Quality Classification Results

To understand whether the considered image quality metrics could indeed help distinguish between high-quality and motion-corrupted image scans, we plotted quality scores for each group (Fig. 3). High-quality scans displayed significantly higher foreground-to-background energy ratios, higher signal-to-noise-ratios, and lower mean background intensities compared to motion-corrupted scans. Even though the entropy-focus criterion

specifically targets motion artefacts, we found no significant differences between the two groups of images in this regard (high-quality: 0.48 [IQR 0.46, 0.50] vs motion-corrupted: 0.47 [IQR 0.46, 0.49]; $p = 0.52$).

We then used a logistic regression model trained on similar images to predict image quality, calculating an AUROC of approximately 0.98. Although entropy-focus criterion values were not significantly different for high-quality and motion-corrupted images, omitting it did not lead to a better model ($AUCROC = 0.96$). Only two scans out of the total 60 (one image of each quality group) were misclassified. Further visual inspection of these two cases revealed increased signal in the background region of the high-quality appearing scan compared to that in the apparently motion-corrupted scan (foreground-to-background energy ratio: 4403.45 vs 4779.42). This finding agrees with what can be perceived via visual inspection (Fig. 4), suggesting that the image labelled as high-quality was corrupted by motion artefacts.

We also compared our approach with one considering texture analysis of brain tissues, described in [6]. The use of motion and noise descriptors led to improved quality control performance when compared to that obtained using Haralick-based textures ($AUROC = 0.98$ with our proposal vs 0.94 with texture analysis). Hence, we used our logistic regression model using motion and noise descriptors to predict image quality.

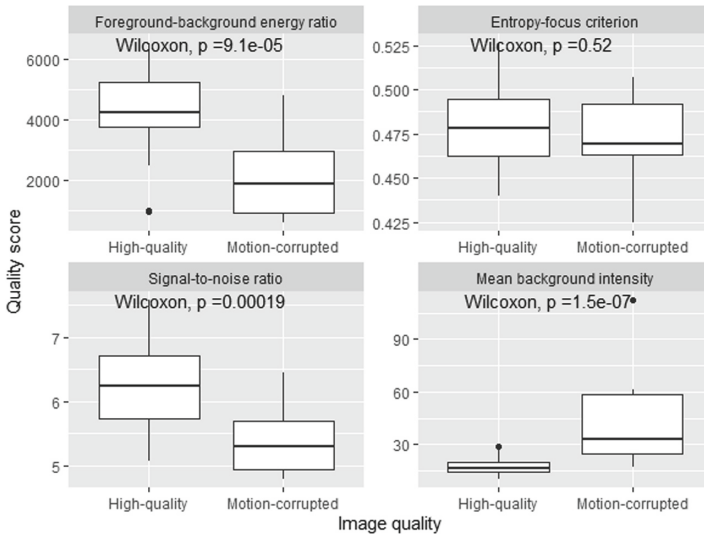


Fig. 3. Image quality scores for high-quality and motion-corrupted T2-w scans. We tested for differences in quality scores using the unpaired two-sample Wilcoxon test.

3.2 Motion Artefact Reduction

We applied the proposed motion artefact reduction method on motion-corrupted scans. The algorithm improves the visual quality of the T2-w images while retaining detail (Fig. 5); in some cases, these features become evident as noise is also reduced.

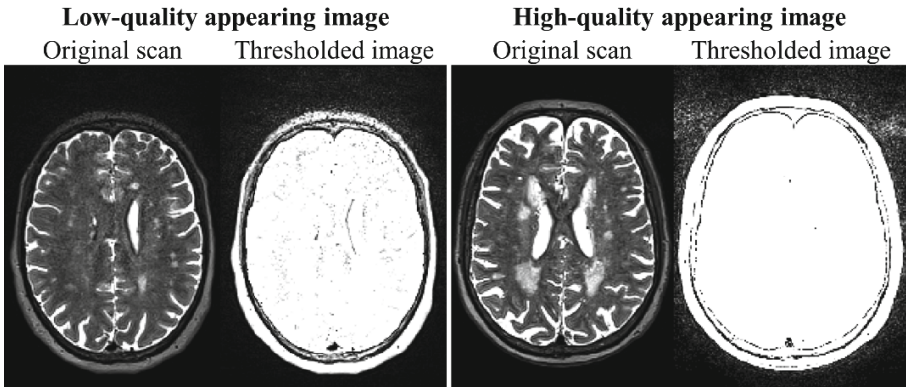


Fig. 4. Images that were misclassified using our logistic regression model. We thresholded intensities above 50 to show the background signal more clearly (thresholded images).

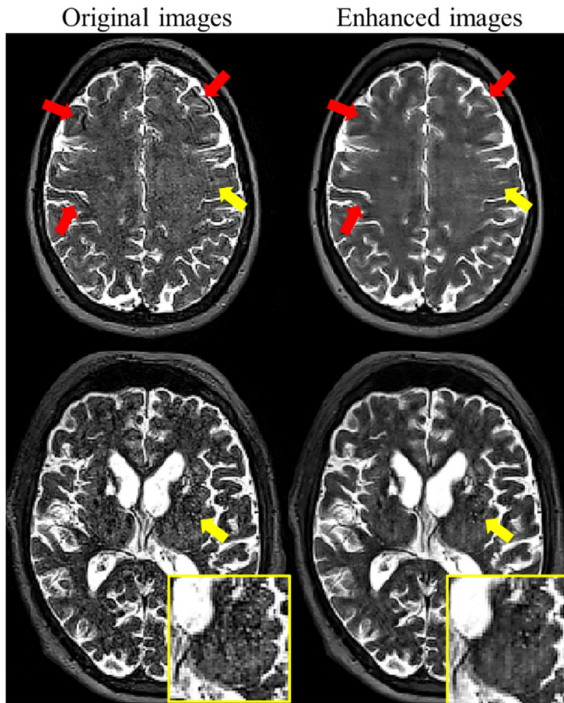


Fig. 5. Original and enhanced scans. Yellow arrows point to regions displaying enlarged perivascular spaces and red ones to evident motion artefacts corrected after image enhancement. (Color figure online)

3.3 Relationship Between Computational Measures and Clinical Visual Scores

We calculated polyserial correlations to assess the relationship between visual and computational PVS measures. We compared correlations obtained when assessing PVS on original scans, those enhanced using the total variation denoising framework [6], and those using our proposed motion artefact reduction (Table 3). Overall, correlation scores increased consistently after selective filtering. The effect was particularly evident in the centrum semiovale where the correlation between visual scores and volume increased from $\rho = 0.17$ (95% CI 0.14, 0.21) to $\rho = 0.29$ (95% CI 0.26, 0.32) and $\rho = 0.86$ (95% CI 0.85, 0.88) using the total variation framework and proposed method, respectively. Furthermore, the relationship between quantitative and qualitative scores was positive once we filtered motion-corrupted images.

Table 3. Polyserial correlations between quantitative and visual measures of perivascular spaces before and after filtering. The higher the correlation, the stronger the relationship between computational and visual scores. We consider the count and volume as quantitative measurements of the presence and enlargement of perivascular spaces. CI: confidence interval. BG: basal ganglia. CSO: centrum semiovale.

	Variable	Original			Total variation in image space [6]			Our proposal		
		ρ	95% CI		ρ	95% CI		ρ	95% CI	
BG	Count	0.38	0.35	0.41	0.43	0.40	0.46	0.50	0.48	0.53
	Volume	0.63	0.61	0.65	0.69	0.67	0.71	0.72	0.71	0.74
CSO	Count	-0.10	-0.13	-0.06	-0.08	-0.05	-0.01	0.34	0.31	0.37
	Volume	0.17	0.14	0.21	0.29	0.26	0.32	0.86	0.85	0.88

Further examination of the computational PVS measurements stratified by clinical visual score and image quality (Fig. 6) suggested the application of the k-space analysis led to more similar estimates between high-quality and image-enhanced scans compared to when no filtering was considered or when filtering in the image space.

4 Discussion

Imaging artefacts limit the applicability of computational solutions, especially those quantifying PVS. This is primarily due to their small size (less than 3 mm) [1] and limitations in imaging technology. We present a computational pipeline for assessing image quality via radiomics analysis and reducing motion artefacts selectively, thus improving PVS segmentation and quantification.

Motion artefacts are a common problem in clinical studies using MRI [11]. Whilst motion may happen occasionally, medical conditions – e.g., strokes [17] – may also cause movement disorders. Alarmingly, the prevalence of motion artefacts limiting computational PVS segmentation has been reported to be as high as 20% [5], a similar proportion to that in our sample. Recovering this data that would otherwise be unusable is therefore

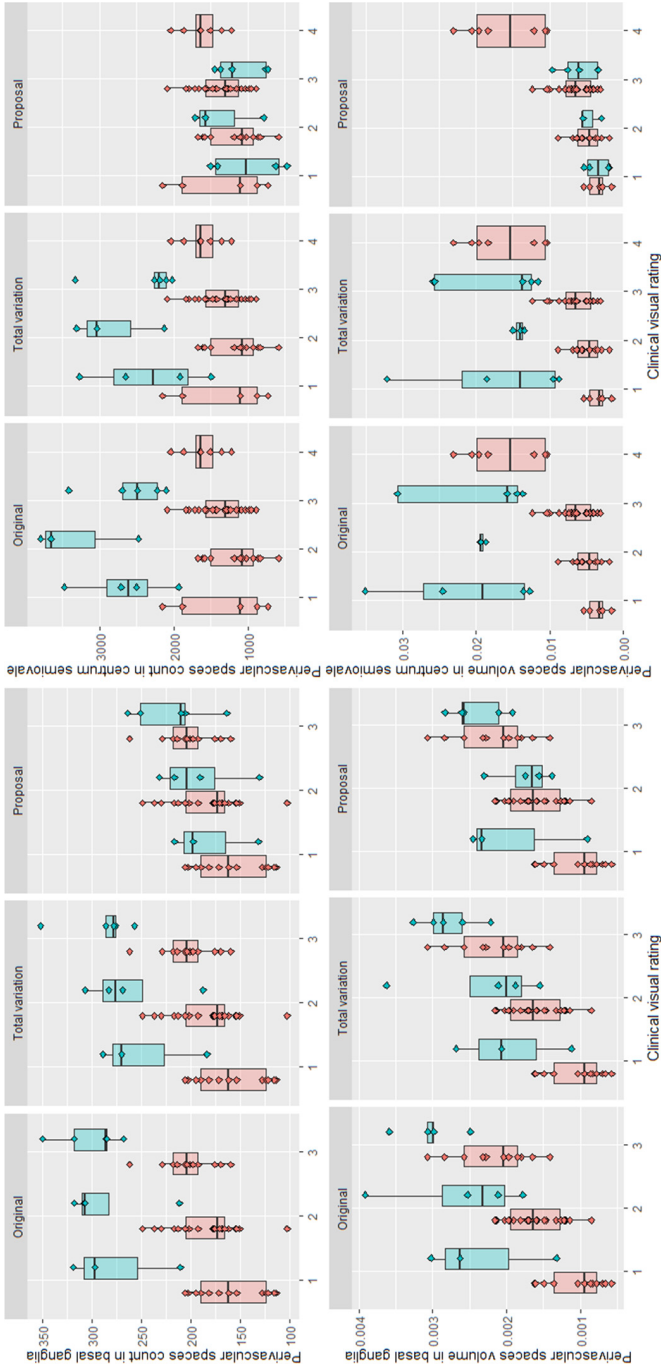


Fig. 6. Perivascular space count and volume quantified in high-quality (pink) and motion-corrupted T2-w scans (green) stratified by clinical visual ratings. The count and volume are computed on original scans as well as those enhanced using the total variation framework and the proposed autofocusing method. We anticipate intra-group similarity irrespective of image quality, i.e., patients with the same visual rating should exhibit similar PVS count and volume and this should not be subject to image quality. (Color figure online)

crucial in the assessment of PVS and further validate their use as biomarker of brain health.

A key step in the proposed pipeline involves separating low- and high-quality scans to avoid blurring the latter unnecessarily as it would otherwise lead to reduced PVS sensitivity [6]. Previous work has shown that this step can be carried out via texture analysis. However, textures extracted from brain tissues reflect both the quality of the scans but also the presence of brain pathologies [9]. Instead, we opted for image quality metrics using background information only or ratios between background and foreground signal to avoid this problem. We tested whether the entropy-focus criterion, foreground-background energy ratio, mean background intensity, and signal-to-noise ratio were appropriate for characterising imaging artefacts in the considered sample.

Our experimental results suggest that the use of image quality metrics permit distinguishing high-quality scans from low-quality ones (AUROC = 0.98) better than texture-based proposals (AUROC = 0.94). Moreover, we observed an image that was originally classified as high-quality was actually corrupted by motion artefacts, supporting the claim that some artefacts evade human detection due to their subtlety or visual fatigue [7]. Automatic image quality control can therefore allow the timely detection of imaging issues that may compromise subsequent processes.

Once we automatically segregated motion-corrupted scans, we proceeded with artefact reduction. Previous work showed filtering in the image space can help to reduce imaging artefacts [6], however, these approximations do not necessarily tackle the primary problem: missing or corrupted k-space measurements. We hypothesise that analysis of the k-space measurements is essential to improve the quality of the images without dispensing with clinically relevant information. In this particular case, T2-w scans were acquired using an elliptical k-space filling trajectory, a technique which oversamples the centre of the k-space [11]. Thus, motion reduction can be achieved by nullifying segments of the k-space displaying, for example, pie-slice [12] or sawtooth patterns. However, these segments need to be re-estimated to prevent a loss in resolution. As a proof of concept, we manually nullified segments of the k-space evidencing these patterns and regressed them using the total variation optimisation framework. We confirmed these segments were indeed linked with motion artefacts since their correction led to increased image quality. Future work should consider automatic detection of these motion-corrupted k-space regions.

Our work has some limitations. First, while nullifying segments of the k-space may work for scans acquired using elliptical trajectories, the same strategy may not be suitable for other types of acquisitions. Approximations using artificial intelligence – e.g., deep learning – may be explored in the future to compensate for these problems in a more generalised way. Moreover, a digital reference object containing PVS and a computational model mimicking image acquisition – similar to the work in [18] – may help to train a model with heterogeneous yet realistic cases, thus preventing potential generalisability issues [19]. Second, we also evaluated our proposal on a relatively small sample of an ongoing prospective study of mild stroke patients. While our results seem encouraging, further validation on a larger dataset containing T1w and T2w imaging sequences acquired with multiple imaging protocols is necessary to determine the suitability of the proposed pipeline for improving PVS quantification. We expect relevant image quality

metrics to differ from those considered in this work, especially if scans are acquired with different k -space trajectories. The outcomes of this experiment could later be compared to descriptors that were found relevant for general automatic quality control [7, 20–23]. Third, statistical analysis of the relationship between computational estimates of PVS burden with demographics and risk factors could complement current analysis, helping to further validate PVS as a biomarker of brain health. Fourth, our proposal offers a partial solution to PVS quantification in motion-corrupted images: reduced false positive rates due to imaging artefact reduction but also reduced true positive rates as k -space extrapolation inevitably blurs some small PVS (e.g., those located in the medial part of the basal ganglia in Fig. 5). Although sharpening filters may improve visual appearance, they do not address the underlying problem: data loss. Motion correction leveraging Fourier transform properties may help to tackle this problem [11], but adjustments may be needed to ensure optimal results in scans acquired using non-Cartesian trajectories.

In conclusion, we have developed a pipeline for evaluating image quality automatically and correct motion artefacts, if needed, to improve PVS quantification. Experimental results suggests our proposal reduces imaging artefacts successfully and leads to a higher correlation between computational and visual measurements of PVS burden. Our development is practical since it helps to recover data otherwise useless and timely given the growing interest in PVS as a potential biomarker of brain dysfunction.

Acknowledgements. This work is supported by: MRC Doctoral Training Programme in Precision Medicine (JB - Award Reference No. 2096671); the UK Dementia Research Institute which receives its funding from DRI Ltd, funded by the UK MRC, Alzheimer’s Society and Alzheimer’s Research UK; the Foundation Leducq Network for the Study of Perivascular Spaces in Small Vessel Disease (16 CVD 05); Stroke Association ‘Small Vessel Disease-Spotlight on Symptoms (SVD-SOS)’ (SAPG 19\100068); The Row Fogo Charitable Trust Centre for Research into Aging and the Brain (MVH) (BRO-D.FID3668413); Stroke Association Garfield Weston Foundation Senior Clinical Lectureship (FND) (TSALECT 2015/04); NHS Research Scotland (FND); British Heart Foundation Edinburgh Centre for Research Excellence (RE/18/5/34216); a British Heart Foundation Chair award (RMT) (CH/12/4/29762); NHS Lothian Research and Development Office (MJT); European Union Horizon 2020, PHC-03-15, project No666881, ‘SVDs@Target’ (MS); Chief Scientist Office of Scotland Clinical Academic Fellowship (UC) (CAF/18/08); Stroke Association Princess Margaret Research Development Fellowship (UC) (2018); Alzheimer Nederland (ACCJ). The Research MR scanners are supported by the Scottish Funding Council through the Scottish Imaging Network, A Platform for Scientific Excellence (SINAPSE) Collaboration; the 3T scanner is funded by the Wellcome Trust (104916/Z/14/Z), Dunhill Trust (R380R/1114), Edinburgh and Lothians Health Foundation (2012/17), Muir Maxwell Research Fund, and the University of Edinburgh. We thank the participants, their families, radiographers at Edinburgh Imaging Facility Royal Infirmary of Edinburgh, and the Stroke Research Network at the University of Edinburgh.

References

1. Potter, G.M., Chappell, F.M., Morris, Z., Wardlaw, J.M.: Cerebral perivascular spaces visible on magnetic resonance imaging: development of a qualitative rating scale and its observer reliability. *Cerebrovasc. Dis.* **39**(3–4), 224–231 (2015)

2. Wardlaw, J.M., Smith, C., Dichgans, M.: Small vessel disease: mechanisms and clinical implications. *Lancet Neurol.* **18**(7), 684–696 (2019)
3. Wardlaw, J.M., et al.: Perivascular spaces in the brain: anatomy, physiology and pathology. *Nat. Rev. Neurol.* **16**(3), 137–153 (2020)
4. del Maria, C., Hernández, V., Piper, R.J., Wang, X., Deary, I.J., Wardlaw, J.M.: Towards the automatic computational assessment of enlarged perivascular spaces on brain magnetic resonance images: a systematic review: computational assessment of perivascular spaces. *J. Magn. Reson. Imaging* **38**(4), 774–785 (2013). <https://doi.org/10.1002/jmri.24047>
5. Ballerini, L., et al.: Computational quantification of brain perivascular space morphologies: associations with vascular risk factors and white matter hyperintensities. A study in the Lothian Birth Cohort 1936. *NeuroImage Clin.* **25**(2019), 102120 (2020)
6. Bernal, J., et al.: A framework for jointly assessing and reducing imaging artefacts automatically using texture analysis and total variation optimisation for improving perivascular spaces quantification in brain magnetic resonance imaging. In: Papież, B.W., Namburete, A.I.L., Yaqub, M., Noble, J.A. (eds.) *MIUA 2020. CCIS*, vol. 1248, pp. 171–183. Springer, Cham (2020). https://doi.org/10.1007/978-3-030-52791-4_14
7. Esteban, O., Birman, D., Schaer, M., Koyejo, O.O., Poldrack, R.A., Gorgolewski, K.J.: MRIQC: advancing the automatic prediction of image quality in MRI from unseen sites. *PLoS ONE* **12**(9), 1–21 (2017)
8. Valdés Hernández, M.d.C., et al.: Application of texture analysis to study small vessel disease and blood–brain barrier integrity. *Front. Neurol.* **8**, 327 (2017)
9. Bernal, J., et al.: Analysis of dynamic texture and spatial spectral descriptors of dynamic contrast-enhanced brain magnetic resonance images for studying small vessel disease. *Magn. Reson. Imaging* **66**, 240–247 (2020)
10. Atkinson, D., Hill, D.L.G., Stoyle, P.N.R., Summers, P.E., Keevil, S.F.: Automatic correction of motion artifacts in magnetic resonance images using an entropy focus criterion. *IEEE Trans. Med. Imaging* **16**(6), 903–910 (1997)
11. Zaitsev, M., Maclaren, J., Herbst, M.: Motion artifacts in MRI: a complex problem with many partial solutions. *J. Magn. Reson. Imaging* **42**(4), 887–901 (2015)
12. Godenschweger, F., et al.: Motion correction in MRI of the brain. *Phys. Med. Biol.* **61**(5), R32–R56 (2017)
13. Lustig, M., Donoho, D., Pauly, J.M.: Sparse MRI: the application of compressed sensing for rapid MR imaging. *Magn. Reson. Med.* **58**(6), 1182–1195 (2007)
14. Lamy, J., et al.: Vesselness filters: a survey with benchmarks applied to liver imaging. In: *International Conference on Pattern Recognition* (2020)
15. Frangi, A.F., Niessen, W.J., Vincken, K.L., Viergever, M.A.: Multiscale vessel enhancement filtering. In: Wells, W.M., Colchester, A., Delp, S. (eds.) *MICCAI 1998. LNCS*, vol. 1496, pp. 130–137. Springer, Heidelberg (1998). <https://doi.org/10.1007/BFb0056195>
16. Ballerini, L., et al.: Perivascular spaces segmentation in brain MRI using optimal 3D filtering. *Sci. Rep.* **8**(1), 1–11 (2018)
17. Handley, A., Medcalf, P., Hellier, K., Dutta, D.: Movement disorders after stroke. *Age Ageing* **38**(3), 260–266 (2009)
18. Bernal, J., et al.: A four-dimensional computational model of dynamic contrast-enhanced magnetic resonance imaging measurement of subtle blood-brain barrier leakage. *Neuroimage* **230**, 117786 (2021). <https://doi.org/10.1016/j.neuroimage.2021.117786>
19. Billot, B., Robinson, E., Dalca, A.V., Iglesias, J.E.: Partial volume segmentation of brain MRI scans of any resolution and contrast. In: Martel, A.L., et al. (eds.) *MICCAI 2020. LNCS*, vol. 12267, pp. 177–187. Springer, Cham (2020). https://doi.org/10.1007/978-3-030-59728-3_18
20. Magnotta, V.A., Friedman, L.: Measurement of signal-to-noise and contrast-to-noise in the fBIRN multicenter imaging study. *J. Digit. Imaging* **19**(2), 140–147 (2006)

21. Kellman, P., McVeigh, E.R.: Image reconstruction in SNR units: a general method for SNR measurement. *Magn. Reson. Med.* **54**(6), 1439–1447 (2005)
22. Dietrich, O., Raya, J.G., Reeder, S.B., Reiser, M.F., Schoenberg, S.O.: Measurement of signal-to-noise ratios in MR images: influence of multichannel coils, parallel imaging, and reconstruction filters. *J. Magn. Reson. Imaging* **26**(2), 375–385 (2007)
23. Mortamet, B., et al.: Automatic quality assessment in structural brain magnetic resonance imaging. *Magn. Reson. Med.* **62**(2), 365–372 (2009)
24. Clancy, U., et al.: Rationale and design of a longitudinal study of cerebral small vessel diseases, clinical and imaging outcomes in patients presenting with mild ischaemic stroke: mild stroke study 3. *Eur. Stroke J.* **6**(1), 81–88 (2020)